Molecular Neurobiology (2019) 56:5608–5625
https://doi.org/10.1007/s12035-019-1491-8

MicroRNA-210 Downregulates ISCU and Induces Mitochondrial Dysfunction and Neuronal Death in Neonatal Hypoxic-Ischemic Brain Injury

Qingyi Ma[1] · Chiranjib Dasgupta[1] · Yong Li[1] · Lei Huang[1] · Lubo Zhang[1]

Received: 20 November 2018 / Accepted: 10 January 2019 / Published online: 17 January 2019
© Springer Science+Business Media, LLC, part of Springer Nature 2019

Abstract

Neonatal hypoxic-ischemic (HI) brain injury causes significant mortality and long-term neurologic sequelae. We previously demonstrated that HI significantly increased microRNA-210 (miR-210) in the neonatal rat brain and inhibition of brain endogenous miR-210 was neuroprotective in HI brain injury. However, the molecular mechanisms underpinning this neuroprotection remain unclear. Using both in vivo and in vitro models, herein we uncover a novel mechanism mediating oxidative brain injury after neonatal HI, in which miR-210 induces mitochondrial dysfunction via downregulation of iron-sulfur cluster assembly protein (ISCU). Inhibition of miR-210 significantly ameliorates mitochondrial dysfunction, oxidative stress, and neuronal loss in the neonatal brain subjected to HI, as well as in primary cortical neurons exposed to oxygen-glucose deprivation (OGD). These effects are mediated through ISCU, in that miR-210 mimic decreases ISCU abundance in the brains of rat pups and primary cortical neurons, and inhibition of miR-210 protects ISCU against HI in vivo or OGD in vitro. Deletion of miR-210 binding sequences at the 3′UTR of ISCU transcript ablates miR-210-induced downregulation of ISCU protein abundance in PC12 cells. In primary cortical neurons, miR-210 mimic or silencing ISCU results in mitochondrial dysfunction, reactive oxygen species production, and activation of caspase-dependent death pathways. Of importance, knockdown of ISCU increases HI-induced injury in the neonatal rat brain and counteracts the neuroprotection of miR-210 inhibition. Therefore, miR-210 by downregulating ISCU and inducing mitochondrial dysfunction in neurons is a potent contributor of oxidative brain injury after neonatal HI.

Keywords Neonatal hypoxia-ischemia · MicroRNA-210 · Mitochondrial dysfunction · Oxidative stress · Neuronal death

Introduction

Hypoxic-ischemic encephalopathy (HIE) is the most common cause of neonatal brain damage resulting from systemic asphyxia that may occur during the perinatal period [1]. HIE causes significant mortality and long-term neurologic sequelae including learning disabilities, mental retardation, seizure, and cerebral palsy [2, 3]. To date, only therapeutic hypothermia provides partially neuroprotective effect in clinic for infants with HIE [4, 5]. Thus, advanced knowledge regarding the molecular mechanisms and pathogenesis of neonatal hypoxic-ischemic (HI) brain injury are of critical importance for the development of effective therapeutic interventions.

Clinical signs in neonates suffered from HIE are associated with a series of excito-oxidative events such as oxidative stress accompanied by activation of neuronal death pathways [6, 7]. Mitochondria play a central role in determining the cellular fate of neurons in the developing brain under stress. Mitochondrial dysfunctions arise very early during neonatal HI, and are associated with excessive generation of toxic free radicals, disruption of oxidative phosphorylation process, and activation of cell death pathways [8–10]. The mitochondria electron transport chain (ETC) is a major source of excessive electrons responsible for the cellular oxidative stress under hypoxic conditions [11]. For example, mitochondrial complex I (NADH dehydrogenase), a key enzyme of ECT facilitating proton translocation, is regarded as one of the main sites of superoxide generation [12, 13]. Mounting evidence shows that complex I deficiency results in neuronal death in various

✉ Qingyi Ma
qma@llu.edu

✉ Lubo Zhang
lzhang@llu.edu

[1] The Lawrence D. Longo Center for Perinatal Biology, Department of Basic Sciences, Loma Linda University School of Medicine, Loma Linda, CA 92350, USA

oxidative stress-related neurological disorders [14, 15]. Relevantly, the activity of complex I is progressively declined within 1 day after the onset of HI in neonates and contributes to increased oxidative stress [9].

We have demonstrated that HI significantly increases microRNA-210 (miR-210) in the neonatal rat brain and inhibition of brain miR-210 with its complementary locked nucleic acid oligonucleotides (miR-210-LNA) provides neuroprotection in neonatal HI brain injury [16]. MiRs are a group of non-coding RNAs with about 21–22 nucleotide long, and function in silencing gene expression by binding to the 3′ untranslated region (3′UTR) of the transcripts of target genes [17, 18]. MiR-210 is the *Master Hypoxamir* of a specific group of miRNAs due to its high hypoxia-inducible characters [19]. One of the downstream targets of miR-210 is iron-sulfur cluster assembly protein (ISCU) [20], which engages in the assembly and transportation of iron-sulfur clusters in mitochondrial complex I enzymes and involves in mitochondrial respiration and energy production [21]. Downregulation of ISCU ultimately disrupts mitochondrial energy metabolism, increases mitochondrial reactive oxygen species (ROS) production, and enhances cell death through the inhibition of complex I [20, 22]. However, the role of the miR-210/ISCU axis in modulating mitochondrial functions in neurons and its impact in neuronal death remains unclear.

Herein, we reveal a novel mechanism that the miR-210/ISCU axis mediates oxidative brain injury by increasing mitochondrial dysfunction in the neonatal brain suffered from HI, as well as in primary cortical neurons exposed to oxygen-glucose deprivation (OGD). We demonstrate that inhibition of miR-210 reduces mitochondrial dysfunction, neuronal oxidative stress, and cell death both in vivo and in vitro. We validate that miR-210 negatively regulates ISCU protein abundance in neurons, and deletion of the miR-210 binding sequences at the 3′UTR of ISCU transcript ablates the action of miR-210. We also reveal that downregulation of ISCU is detrimental to the neonatal brain, and counteracts neuroprotective effect of miR-210 inhibition after HI. Moreover, in primary cortical neurons, functions of miR-210 and ISCU are convergent in modulating mitochondrial electron transport and ROS generation.

Materials and Methods

Antibodies and Chemicals

Primary antibodies used in this study included the following: ISCU (14812-1-AP, Proteintech); FLAG (F1804-50UG, Sigma-Aldrich); 3-Nitrotyrosine (ab52309, Abcam; SAB5200009, Sigma-Aldrich); 4 Hydroxynonenal (ab46545, Abcam); MAP 2 (ab32454, Abcam); NeuN (MAB 377, Millipore); β-actin (A1978, Sigma-Aldrich); GAPDH (ab9485, Abcam). Secondary antibodies used for immunofluorescence and immunocytochemistry were purchased from Invitrogen, including Alexa Fluor 594 anti-mouse (A-21203), Alexa Fluor 594 anti-rabbit (A-21207), Alexa Fluor 488 anti-mouse (A-21202), and Alexa Fluor 488 anti-rabbit (A21206). All secondary antibodies using for western blot were purchased from Santa Cruz Biotechnology. DAPI (D1306) for nuclear staining was purchased from Invitrogen. Cresyl Violet (C5042) for Nissl staining and paraformaldehyde (PFA) were obtained from Sigma-Aldrich. Tissue-Tek OCT (25608-930) was purchased from VWR. Donkey serum (017-000-121) was purchased from Jackson ImmunoResearch. MicroRNA-210 mimic (MSY0000881) and ALLStars negative control (SI03650318) were purchased from Qiagen. MicroRNA-210-LNA (4103837-102) and scramble (199006-102) were purchased from Exiqon. Stealth ISCU siRNAs (set of three, RSS353218, RSS353219, RSS353220) (1330001) were purchased from Fisher Scientific. Unless stated otherwise, the materials for cell cultures were purchase from Invitrogen. Horse serum (30-2040) was purchased from ATCC. Poly-D-lysine (P7886-500MG), Ara-C (C6645), and DNase (D4513) were obtained from Sigma-Aldrich. The p3XFLAG-CMV™-7.1 expression vector (E7533-20UG) and 2,3,5-triphenyltetrazolium chloride (TTC, T8877) were purchased from Sigma-Aldrich. TRIzol reagent (15596026) was purchased from Invitrogen. RIPA lysis buffer (sc-24948) was purchased from Santa Cruz Biotechnology.

Neonatal Rat Model of Hypoxia-Ischemia

A modified Rice-Vannucci model was produced in 7-day-old (P7) CD1 rat pups as described previously [16, 23]. Briefly, rat pups (Charles River Laboratories) were fully anesthetized with inhalation of 2–3% isoflurane. The right common carotid artery (CCA) in the neck was exposed, double ligated with a 5.0 silk surgical suture, and then cut between two ligation sites. After surgery, pups were recuperated on a heating pad at 37 °C for 1 h, and then placed in a hypoxic incubator containing humidified 8% oxygen balanced with 92% nitrogen at 37 °C for 1.5 h. At the end of hypoxia, pups were returned to their dams for recovery. For the sham group, the right common carotid artery of rat pup was exposed but without ligation and hypoxia. Rat pups of mixed males and females were randomly assigned into each experimental group. All procedures and protocols were approved by the Institutional Animal Care and Use Committee of Loma Linda University and followed the guidelines by the National Institutes of Health Guide for the Care and Use of Laboratory Animals.

Intracerebroventricular Injection and Experimental Design

Compounds with the total volume of 2 μl were stereotaxically injected into the ipsilateral hemisphere of rat pups

intracerebroventricularly (placement coordinates: 2 mm posterior, 1.5 mm lateral, 3 mm below the skull surface) with a flow rate of 0.5 μl/min, as described previously [16].

MiR-210-LNA (4103837-102, Exiqon) and LNA scramble control (199006-102, Exiqon) were prepared according to the manufacturer's instructions. Either miR-210-LNA (100 pmol in 2 μl) or its negative control was delivered 4 h after neonatal HI via intracerebroventricular (*i.c.v.*) injection. The treatment regimen of miR-210-LNA was determined in our previous study, in which miR-210-LNA with this dosage showed neuroprotective effect [16].

MiR-210 mimic (MSY0000881, Qiagen) and ALLStars negative control (SI03650318, Qiagen) were prepared according to the manufacturer's instructions. Either miR-210 mimic (100 pmol in 2 μl) or its negative control was injected into the brains of P5 rat pups, and brain samples were collected 48 h after injection. The treatment regimen of miR-210 mimic was determined in our previous study, in which miR-210 mimic with this dosage significantly downregulated the expression of target genes [16, 24].

Stealth siRNAs (set of three; RSS353218, RSS353219, RSS353220) (1330001) targeting ISCU gene and control siRNA were obtained from Fisher Scientific. The siRNA is a pool of three 25-nt siRNAs designed to knockdown gene expression targeting different ISCU exons, and was prepared according to the manufacturer's instructions. The sequences of rat ISCU siRNAs were as follows: sequence 1: 5′-CAAG AAGGUUGUGGAUCAUUAUGAA-3′; sequence 2: 5′-CCGGCAUGUGGUGACGUCAUGAAAC-3′; sequence 3: 5′-AAACAUUUGGCUGCGGCUCCGCCAU-3′. Either ISCU siRNAs (100 pmol in 2 μl) or negative control was administered into the brains of P5 rat pups via *i.c.v.* injection. Some animals were sacrificed for ISCU mRNA or protein expression assay, and some animals were subjected to HI 48 h after injection.

Measurement of Brain Infarct Size

Brain infarct size was determined 48 h after HI using 2,3,5-triphenyltetrazolium chloride monohydrate (TTC; T8877, Sigma-Aldrich) staining as described previously [24, 25]. Briefly, the brain was isolated from each pup, dissected into coronal sections (2 mm thickness, 5 slices per brain), and immersed into pre-warmed 2% TTC in 0.1 M phosphate-buffered saline (PBS, pH 7.4) at 37 °C for 5 min against light. Sections were washed with PBS and then fixed by 10% formaldehyde overnight. The caudal and the rostral surfaces of each slice were photographed using a digital camera, and the percentage of infarct area (average of both sides) in the ipsilateral hemisphere for each slice was traced and analyzed by NIH Image J software.

Mitochondria Isolation from Brain Tissue

Brain mitochondria were isolated using a mitochondria isolation kit for tissue (89801, Invitrogen) according to the manufacturer's instructions. The brain was extracted from each rat pup and separated into ipsilateral or contralateral cerebral hemisphere. Only the ipsilateral cerebral hemisphere was used for mitochondria isolation. Briefly, samples were washed with ice-cold PBS, cut into small pieces in a mixture of bovine serum albumin (BSA) and mitochondria isolation reagent A solution with protease inhibitor, and then homogenized using a pre-chilled Dounce tissue grinder on ice. After mixing with mitochondria isolation reagent C, the homogenized mixtures were centrifuged at 700×*g* at 4 °C for 10 min. The supernatants were collected and further centrifuged at 3000×*g* at 4 °C for 15 min. The pellets were saved as mitochondria fraction and used for complex I activity assay or western blot.

Immunofluorescence and Nissl Staining

Rat pups were transcardially perfused with ice-cold 0.1 M PBS (pH 7.4) followed by 4% PFA (Sigma-Aldrich). The brain was post-fixed in 4% PFA overnight, dehydrated with 30% sucrose solution in PBS at 4 °C, and allowed to completely sink to the bottom of the container. Then samples were dissected, embedded into Tissue-Tek optimal cutting temperature compound (OCT) (25608-930, VWR) on dry ice, and cryosectioned at a thickness of 20 μm for immunofluorescence staining or 10 μm for Nissl staining using CM3050S cryostat (Leica Microsystems). Slices were blocked with 5% donkey serum (017-000-121, Jackson ImmunoResearch) containing 0.3% Triton X-100 (Sigma-Aldrich) at room temperature for 1 h, then incubated with the following primary antibodies at 4 °C overnight: rabbit anti-MAP 2 polyclonal antibody (ab32454, Abcam); mouse anti-NeuN monoclonal antibody (MAB377, Millipore); mouse anti-3-nitrotyrosine monoclonal antibody (SAB5200009, Sigma-Aldrich); rabbit anti-4-hydroxynonenal polyclonal antibody (ab46545, Abcam). After washed with PBS, Alexa Fluor conjugated secondary antibodies, including Alexa Fluor 594-conjugated donkey anti-mouse (A-21203, Invitrogen), Alexa Fluor 594-conjugated donkey anti-rabbit (A-21207, Invitrogen), Alexa Fluor 488-conjugated donkey anti-mouse (A-21202, Invitrogen), or Alexa Fluor 488-conjugated donkey anti-rabbit (A21206, Invitrogen), were incubated with brain slices at room temperature for 1 h. After washed, tissue slices were mounted and coverslipped with fluorescent mounting media (S3023, Dako). All slices were scanned with Zeiss LSM 710 NLO confocal microscope (Zeiss). For Nissl staining, slides with mounted slices were immersed into 1% Cresyl Violet solution (Sigma-Aldrich) followed by dehydration in graded ethanol solutions, and then coverslipped with Permount (Fisher Scientific). Images were taken using Zeiss Axio Imager A1 upright microscope (Zeiss). All the images

were analyzed using NIH Image J version 1.41 software. Microscopes were provided by Advanced Imaging and Microscopy Facility of Center of Perinatal Biology.

Primary Cortical Neuron Isolation and Culture

Primary cortical neurons were prepared from early postnatal (P0) rat pups of either sex as previously described [26, 27]. Briefly, the cerebral cortex from P0 rat pups was removed into HBSS buffer (Fisher Scientific) and dissociated with 0.25% trypsin (25200072, Fisher Scientific) and DNAse (D4513, Sigma) at 37.0 °C water bath for 15 min. After trituration with fire-polished Pasteur pipettes, dissociated cells were suspended in Neurobasal medium (21103049, Invitrogen) supplemented with 2% B27 (17504044, Invitrogen), 1% GlutaMAX (100×; 35050061, Invitrogen) and 100 units/ml penicillin/streptomycin (15140163; Invitrogen), and run through a 40-μm cell strainer (Fisher scientific). Cell suspensions were then plated on poly-D-lysine solution (PDL, 0.1 mg/ml in Boric acid buffer; P7886-500MG, Sigma-Aldrich)-coated 6-well plates (Corning) or 96-well plates (Corning) for biochemical experiments, or on PDL-coated German 12 mm glass coverslips (Fisher scientific) in 24-well plates (Corning) for immunocytochemistry staining at 200–400 cells/mm^2, and maintained in a CO_2 incubator (5% CO_2, 21% O_2) at 37 °C. At day 2 of in vitro culture (DIV2), 2 μM cytosine β-D-arabinofuranoside hydrochloride (Ara-C; C6645, Sigma), an inhibitor of DNA replicate, was added into culture medium to inhibit non-neuronal cell proliferation. Half of the culture medium was replaced every 2–3 days. Experiments were conducted at DIV 5–7, when cultures consisted primarily of neurons (approximately 90% MAP 2-positive cells by immunocytochemistry staining).

Cortical Neuron Transfection

Primary cortical neurons at DIV 5 were transfected with miR-210 mimic (100 nM; Qiagen) or the pool of Stealth ISCU siRNAs (100 nM; Fisher Scientific) using Lipofectamine 2000 (11668027, Invitrogen) in Neurobasal medium (Invitrogen) according to the manufacturer's instructions. The same amount of miR-210 ALLStars negative control or siRNA control with matching GC content was used as negative controls. All experiments were performed 48–72 h after transfection. To test the effect of miR-210 inhibition during OGD, either miR-210-LNA (Exiqon) or LNA scramble control (Exiqon) was transfected 24 h prior to exposure to OGD.

Oxygen-Glucose Deprivation and Lactate Dehydrogenase Assay

Primary cortical neurons were subjected to OGD insult as previously reported [27–31]. Briefly, the neuron culture media were replaced with pre-warmed glucose-deprived Neurobasal-A medium (A2477501, Invitrogen), and then neuron cells were cultured in an incubator filled with 1% oxygen (5% CO_2/95% N_2) at 37 °C for 1.5 or 6 h. At the end of hypoxia, the OGD media were changed to Neurobasal medium supplemented with 2% B27, 1% GlutaMAX (100×), and 100 units/ml penicillin/streptomycin, returned to normal culture condition, and incubated till 24 h (reoxygenation). The degree of cell injury at the end of reoxygenation was assessed by determining the amount of lactate dehydrogenase (LDH) released into the culture medium using the Pierce™ LDH Cytotoxicity assay kit (88954, Fisher Scientific) according to the manufacturer's instructions. The background signal (absorbance at 630 nm) was subtracted from reaction signal (absorbance at 490 nm). LDH release was normalized to protein concentration and the results were shown as fold changes over normal controls.

Plasmid Constructs and Transfection of PC12 Cells

Full length (883 base pairs; intact 3′UTR; ISCU-FL) or fragment (504 base pairs; 3′UTR deletion; ISCU-3′UTR(−)) of *Rattus norvegicus* of ISCU was cloned from brain-derived cDNA and inserted into p3XFLAG-CMV™-7.1 expression vector (E7533-20UG, Sigma-Aldrich) between the EcoRI and HindIII sites. Primers (IDT) used to amplify ISCU-FL were 5′-ATGGCGGCGGCTGGAGCGGG-3′ (forward); 5′-TAGAGAAAACCATCGTCTTCCATTT-3′ (reverse). Primers used to amplify ISCU-3′UTR(−) were 5′-ATGG CGGCGGCTGGAGCGGG-3′ (forward); 5′-TCAC TGCTTCTCCGGCTCGTC-3′ (reverse). All the constructs were confirmed by DNA sequencing to exclude potential PCR-introduced mutations. Rat PC12 cells (ATCC) were maintained in DMEM supplemented with 10% horse serum, 5% fetal bovine serum, and penicillin/streptomycin. The plasmids alone or accompanied with either miR-210 mimic or miR-210 scramble (Neg. Ctrl.) were transfected into PC12 cells with Lipofectamine 2000 (11668027, Invitrogen) in Opti-MEM medium (31985070, Fisher Scientific) according to the manufacturer's instructions. Medium was refreshed at 5–6 h after transfection to reduce the toxicity. PC12 cells cultured on PDL-coated 6-well plate were collected for western blot assay, or on PDL-coated German 12 mm glass coverslips (Fisher scientific) in 24-well plates (Corning) for immunocytochemistry staining. All the experiments were carried out 48 h after transfection.

Measurement of MiR-210

The levels of miR-210 were detected as we previously described [16]. Total RNA was extracted using the TRIzol reagent (15596026; Invitrogen). MiR-210 levels were analyzed by miScript II RT kit (218161, Qiagen) and miScript SYBR

Green PCR kit (218073, Qiagen) with miScript Primer Assay kit (MS00000644, Qiagen) according to the manufacturer's instructions. Briefly, 1 μg of template RNA was mixed with reverse transcription master mix in a final volume of 20 μl and incubated for 60 min at 37 °C, and then the reaction was stopped at 95 °C. Two nanograms of template cDNA was used for miR-210 quantification in a final volume of 25 μl system containing specific primers and QuantiTect SYBR Green PCR master mix according to the manufacturer's instructions. Primers included miScript Universal Primer, miR-210 miScript Primer Assay, and SNORD61 miScript Primer Assay (MS00033705, Qiagen). PCR was done in triplicate and threshold cycle numbers were averaged for each sample. The relative expression levels of mature miR-210 were calculated using the formula $2(^{-\Delta\Delta Ct})$ and normalized to SNORD61. The change of miR-210 was expressed as fold of normal control.

qRT-PCR of ISCU mRNA Quantification

Total RNA was subjected to reverse transcription with Superscript III First-Strand Synthesis System (18080051, Invitrogen), following the manufacturer's instructions. The ISCU mRNA abundance was determined with real-time PCR using iQ SYBR Green Supermix (1708880, Bio-Rad) as we previously described [16]. Primers included the following: ISCU, Forward: TGAAACTGCAGATCCAGGTG; Reverse: TTTTCCCCTTTACCCACT. Actin: Forward: TCAGGTCATCACTATCGGCAAT; Reverse: ACTGTGTT GGCATAGAGGTCTT. Real-time PCR was performed in a final volume of 25 μl and each PCR reaction mixture consisted of specific primers and iQ SYBR Green Supermix. PCR was done in triplicate and threshold cycle numbers were averaged for each sample. The relative expression levels were calculated using the formula $2(^{-\Delta\Delta Ct})$ and normalized to Actin. The change of ISCU was expressed as fold of normal control.

Western Blotting

Western blotting was performed as described previously [16, 32]. Animals were euthanized at indicated time after neonatal HI. The brain was separated into ipsilateral or contralateral hemisphere, and stored at − 80 °C immediately until analysis. Protein extraction was obtained by gently homogenization in RIPA lysis buffer (sc-24948, Santa Cruz Biotechnology) with further centrifugation at 14,000×*g* at 4 °C for 30 min. The supernatant was collected, and the protein concentration was determined using a detergent compatible assay (Bio-Rad). Equal amounts of protein were loaded on an SDS-PAGE gel. After being electrophoresed and transferred to a nitrocellulose membrane, the membrane was blocked and incubated with the primary antibody at 4 °C overnight. The primary antibodies included the following: rabbit polyclonal anti-ISCU antibody (14812-1-AP, Proteintech), mouse monoclonal anti-3-nitrotyrosine antibody (ab52309, Abcam), mouse monoclonal anti-FLAG® M2 antibody (F1804, Sigma-Aldrich), mouse monoclonal anti-β-actin (A1978, Sigma-Aldrich), or rabbit polyclonal anti-GAPDH antibody (ab9485, Abcam). Nitrocellulose membranes were incubated with secondary antibodies (Santa Cruz Biotechnology) for 1 h at room temperature. Immunoblots were then probed with an ECL Plus chemiluminescence reagent kit (32132, Fisher Scientific) and visualized with the imagine system (Bio-Rad, Versa Doc, model 4000). The data were analyzed by the NIH Image J version 1.41 software.

Immunocytochemistry

Cortical neurons or PC12 cells grown on PDL-coated glass coverslips were washed once with ice-cold PBS, and then fixed with 4% PFA for 10 min. After permeabilization with 0.3% Triton X-100 in PBS for 10 min and blocked with 5% donkey serum in PBS for 30 min, cells were then incubated with primary antibodies in blocking solution at 4 °C overnight. The primary antibodies included rabbit anti-MAP 2 polyclonal antibody (Abcam) and mouse anti-FLAG® M2 monoclonal antibody (F1804, Sigma). After washed with PBS, cells were incubated with Alexa Fluor 488-conjugated donkey anti-mouse, Alexa Fluor 594-conjugated donkey anti-rabbit, or Alexa Fluor 488-conjugated donkey anti-rabbit secondary antibody for 1 h at room temperature. All secondary antibodies were purchased from Invitrogen. The nuclear was stained with DAPI (D1306, Invitrogen). After washed, coverslips with cells were mounted on slides using fluorescent mounting media (Dako). All slides were scanned with a Zeiss LSM 710 NLO confocal microscope (Zeiss) in Advanced Imaging and Microscopy Facility of Center of Perinatal biology and analyzed using the NIH Image J version 1.41 software.

Imaging of Intracellular and Mitochondrial ROS

CellROX™ Green Reagent (C10444, Invitrogen) was used to detect intracellular ROS in primary cortical neurons according to the manufacturer's instructions. CellROX® Green reagent is a cell-permeant DNA dye, which is non-fluorescent in reduced state. When oxidized by ROS, this reagent shows strong green fluorescence with absorption/emission maxima of ~485/520 nm and binds to DNA. Therefore, its signal is primarily localized in the nucleus and mitochondria. MitoSOX Red (M36008, Invitrogen), a mitochondrial permeable fluorogenic dye that can emit red fluorescence upon oxidation, was used to detect mitochondrial superoxide in primary cortical neurons according to the manufacturer's instructions. Briefly, cortical neurons were cultured on PDL-coated

12 mm glass coverslips in 24-well plates. After treatments, cells were washed with pre-warmed growth medium, and then incubated with CellROX Green at a final concentration of 5 μM at 37 °C for 30 min, or MitoSOX Red at a final concentration of 5 μM at 37 °C for 10 min. Then neurons were briefly washed with PBS followed by immunostaining with mouse anti-MAP-2 monoclonal antibody (Abcam) and nuclear staining with DAPI. The CellROX fluorescence was obtained with the EVOS Cell Imaging Systems (Invitrogen) and analyzed using NIH image J version 1.41 software. The fluorescence density was normalized to numbers of MAP 2-positive cells. Three independent experiments in duplicate were used for MAP 2-positive cell counting and CellROX fluorescence density analysis. Eight images from each coverslip were taken with ×20 objective. The images of MitoSOX dye were obtained using Zeiss LSM 710 NLO confocal microscope (Zeiss) and analyzed using the NIH Image J version 1.41 software.

Luminescent Assays for ATP Level and Caspase Activities

ATP levels were quantified by the CellTiter-Glo luminescent assay kit (PR-G7570, Promega) according to the manufacturer's instructions. The ATP standard curve was generated using serial tenfold dilutions of ATP disodium salt (A2383, Sigma). The luminescence level was record by luminescence microplate reader (BioTek Instruments). ATP level was analyzed and normalized to total protein from cells treated identically in a replicate plate. Caspase 3/7 and Caspase 9 activities were quantified using the Caspase-Glo 3/7 (G8091, Promega) and Caspase-Glo 9 assay kits (G8211, Promega) according to the manufacturer's instructions. The luminescence level was recorded by luminescence microplate reader (BioTek Instruments) and normalized to total protein concentration from cells treated identically in a replicate plate. The relative caspase activities were expressed as fold changes over the negative controls.

Complex I Activity Assay

Mitochondrial complex I activity was detected by Complex I Enzyme Activity Microplate Assay Kit (ab109721, Abcam) according to the manufacturer's instructions. Raw mitochondria isolations from brain tissue were solubilized in 1% detergent (lauryl maltoside) and centrifuged at 12,000×*g* for 20 min. The supernatants were collected and diluted in incubation solution. A certain amount of protein per well was loaded in a 96-well microplate coated with anti-mitochondrial NADH dehydrogenase antibody and incubated for 3 h at room temperature. The degree of oxidation of NADH to NAD+ by the immunocaptured complex I was determined by the rate of increase in absorbance (mOD/min) at 450 nm. The kinetic analysis is linear over 30 min with 60 s intervals to determine maximum rate of increase using a microplate reader (BioTek Instruments). The relative complex I activity was expressed as fold changes over the controls.

Intracellular Oxidative Stress Assay

Cortical neurons were seeded in PDL-coated 96-well plates. Total intracellular ROS in cortical neurons were measured using the Oxiselect™ in vitro ROS/RNS assay kit (STA347; Cell Biolabs) according to the manufacturer's instructions. Cells were incubated with 2′,7′-dichlorofluorescin diacetate (DCFHDA) for 30 min, and then lysed in 100 μl of 0.3% Triton X-100 in PBS. The relative fluorescence of each well and the 2′,7′-dichlorodihydrofluorescein (DCF) standard were read at 480 nm excitation/530 nm emissions using fluorescence microplate reader (BioTek Instruments). The concentration of the total ROS/RNS was calculated by comparison with the DCF standard curve, and normalized to protein concentrations of each well.

Statistical Analysis

Data were expressed as mean ± standard error of the mean (SEM). All graphs in this study were generated with GraphPad Prism 5. In experiments related to animals, experimental number (n) represents neonates from different dams. All in vitro experiments were performed at least three times. Comparisons between two groups were analyzed using Student's *t* test (unpaired, two-tailed), and multiple comparisons were analyzed using one-way ANOVA following by Newman-Keuls post hoc test. A p value less than 0.05 was considered significant.

Results

Inhibition of miR-210 Reduced Oxidative Stress and Neuron Loss After Neonatal HI Brain Injury

To investigate whether inhibition of miR-210 could ameliorate mitochondrial dysfunction after neonatal HI, either miR-210-LNA or LNA scramble (Neg. Ctrl) was delivered into the ipsilateral hemisphere of P7 rat pups via *i.c.v.* injection 4 h after HI. Twelve hours later, the ipsilateral cerebral hemisphere was collected for isolation of mitochondria and measurement of complex I activity. In isolated mitochondria, a significant reduction of more than 40% in complex I activity was observed in HI animals over the sham. There was no protection observed in Neg. Ctrl animals, which showed about 39% reduction over the sham similar to HI animals. Remarkably, only 16% reduction of complex I activity was observed in miR-210-LNA-treated animals (Fig. 1a).

Complex I is an elemental component for mitochondrial functions; thus, this result indicates that mitochondrial dysfunction occurs acutely following HI, and inhibition of brain endogenous miR-210 protects mitochondrial function against HI.

We then evaluated the antioxidative effect of miR-210 inhibition in neonatal HI brain injury. The 3-nitrotyrosine (3-NT) is an oxidation product and is formed by interactions between oxidant, such as superoxide or reactive nitrogen intermediates, and proteins with tyrosine residue [33]. We visualized 3-NT protein abundance in cortical regions surrounding the infarct in the ipsilateral hemisphere 24 h after HI using immunofluorescence staining on brain slices. The result showed that strong 3-NT fluorescence (red) was observed in MAP 2-positive neurons (green) in the cortex of ipsilateral hemisphere in HI alone or with Neg. Ctrl treatment, which was reduced with miR-210-LNA treatment (Fig. 1b). In

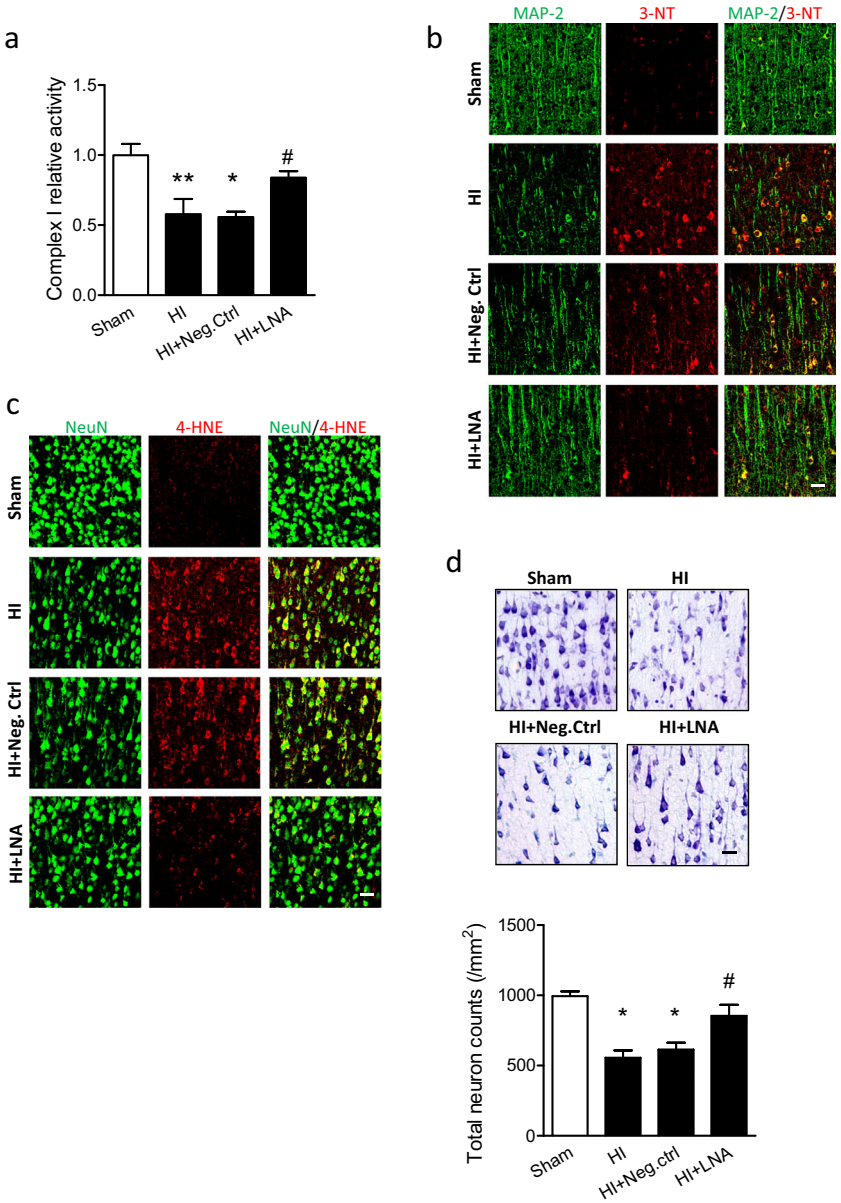

Fig. 1 Inhibition of miR-210 reduces oxidative stress and neuronal loss after neonatal HI. Neonatal HI brain injury was induced in postnatal day 7 (P7) rat pups, and 100 pmol miR-210-LNA or scramble LNA (Neg. Ctrl) was administered into the ipsilateral hemisphere via *i.c.v.* injection 4 h after HI. **a** Complex I activity in isolated mitochondria of the ipsilateral cerebral hemisphere of the brain 12 h after HI. Data are expressed as mean ± SEM. $n = 5$ pups/group in Sham; $n = 6$ pups/group in other groups. *, $p < 0.05$, ** $p < 0.005$ vs Sham, #, $p < 0.05$ vs HI + Neg. Ctrl. ANOVA following by Newman-Keuls post hoc test. **b, c** Representative confocal images of the colocalization of 3-nitrotyrosine (3-NT) (**b**, red), or 4-hydroxynonenal (4-HNE) (**c**, red) with neuron markers (**b**, MAP 2; **c**, NeuN, green) in cortical regions surrounding the infarct in the ipsilateral hemisphere of the brain 24 h after HI. Scale bar, 20 μm. **d** Representative images of Nissl staining and quantification (3 sections/pup, $n = 4$ pups/group) showing neuronal density in cortical regions surrounding the infarct in the ipsilateral hemisphere of the brain 48 h after HI. Scale bar, 20 μm. *, $p < 0.05$ vs Sham, #, $p < 0.05$ vs HI + Neg. Ctrl. ANOVA following by Newman-Keuls post hoc test

addition, 4-hydroxy-2-nonenal (4-HNE) (red), another marker of oxidative stress formed by lipid peroxidation [34], was also visualized in neurons (NeuN, green) in the cortex, and followed the same trend as 3-NT (Fig. 1c). Both 3-NT and 4-HNE were neuronal death inducer [34–36]. Nissl staining showed that severe neuronal loss was induced by HI in the cortex of ipsilateral hemisphere. Accordingly, miR-210-LNA, but not Neg. Ctrl treatment significantly diminished neuron loss from HI (Fig. 1d). Together, these results suggest that inhibition of miR-210 reduces mitochondrial dysfunction, oxidative stress, and neuronal loss after neonatal HI.

Inhibition of miR-210 Reduced Oxidative Stress and Preserved Primary Cortical Neuron Viability from OGD

As the in vivo data demonstrated the antioxidative effect of miR-210-LNA, using isolated primary cortical neurons, we evaluated whether inhibition of miR-210 provided neuroprotection by reducing oxidative stress in an OGD model in vitro. We opted for OGD model as it has long been established to induce hypoxic-ischemic events in primary neurons through optimizing the duration of OGD treatment, and the reoxygenation after OGD also mimics the reperfusion process after HI [37, 38]. First, to determine whether OGD stimulates upregulation of miR-210 in primary cortical neurons, cell cultures at DIV5–7 were exposed to different durations (1.5 or 6 h) of OGD insult. Control cells (normal) were cultured in normal condition for the same durations. Compared with the controls, OGD treatment for 1.5 or 6 h upregulated miR-210 levels by 2.7-fold and 3.1-fold in cortical neurons, respectively (Fig. 2a). There was no statistical difference of miR-210 levels between two durations of OGD treatment, and therefore the protocol of 1.5 h of OGD was used in the rest of experiments. Interestingly, miR-210 levels were also gradually accumulated in primary cortical neurons from 2.7-fold at 0 h to 5.2-fold at 6 h during reoxygenation compared with the normal controls (Fig. 2b), suggesting the reperfusion process also stimulated miR-210 expression in cortical neurons, which may play an important role in reperfusion injury after HI. Thus, these results substantiate our previous finding that miR-210 was time-dependently upregulated in the neonatal brain following HI [16].

We next evaluated whether the inhibition of miR-210 protected primary cortical neuron viability during OGD. Cells were treated with 50 μM miR-210-LNA or scramble LNA (Neg. Ctrl) for 24 h, and then were subjected to OGD followed by reoxygenation. As predicted, miR-210-LNA significantly reduced miR-210 levels by about 60% 6 h after the OGD treatment, compared with Neg. Ctrl (Fig. 3a). Moreover, consistent with the in vivo result (Fig. 1a), OGD/reoxygenation significantly reduced mitochondrial complex I activity in cortical neurons, which was rescued by miR-210-LNA, but not Neg. Ctrl (Fig. 3b). To evaluate the cell viability, the culture medium was collected at the end of OGD/reoxygenation for measuring LDH release. As shown in Fig. 3c, OGD/reoxygenation significantly increased LDH release by about 3.3-fold, indicating the damaged cellular integrity and decreased cell viability. The presence of miR-210-LNA significantly reduced LDH release to 1.5-fold over the normal controls, compared with about 3.2-fold with the presence of Neg. Ctrl (Fig. 3c). Moreover, the activities of caspase 3 and caspase 9 in cortical neurons were significantly upregulated by OGD/reoxygenation, which were inhibited by miR-210-LNA, but not Neg. Ctrl (Fig. 3d, e). As inhibition of miR-210 rescued mitochondrial complex I and reduced neuronal oxidative damage in the neonatal brain after HI (Fig. 1), we then detected the role of miR-210 in modulating ROS production in cortical neurons after OGD/reoxygenation. CellROX, an intracellular ROS dye, was incubated with primary cortical neurons at the end of OGD/reoxygenation. Cells were then fixed and immunostained for a neuron marker MAP 2. The microscopy analysis showed that brighter ROS fluorescence (green) was observed in the nucleus of MAP 2-positive neurons (red) in the control or scramble-treated cells after OGD/reoxygenation, whereas ROS fluorescence was reduced in miR-210-LNA-treated cells (Fig. 3). The following quantification of the fluorescence density of CellROX in MAP 2-positive cells showed a significant 8.7-fold increase of neuronal ROS in OGD/reoxygenation compared with the normal controls. The presence of miR-210-LNA (3.2-fold over Normal) resulted in a significant 62% reduction of ROS, compared with Neg. Ctrl (8.5-fold over Normal) after OGD/

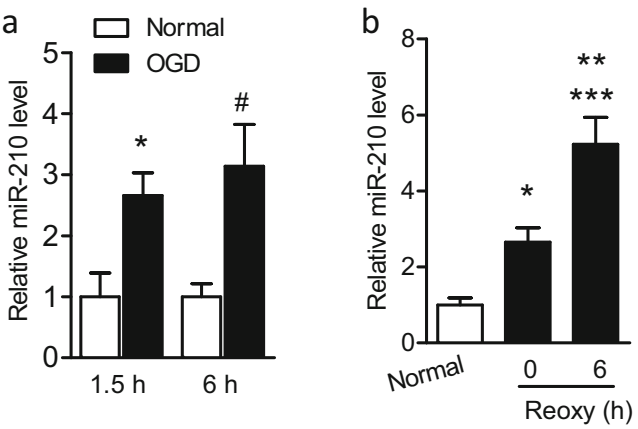

Fig. 2 Upregulation of miR-210 in primary cortical neurons in response to OGD/reoxygenation. **a** Rat primary cortical neurons were subjected to OGD or cultured in normal condition for 1.5 or 6 h. The level of miR-210 level was measured by RT-PCR. Data are expressed as mean ± SEM. $n \geq 3$ independent experiments. *, $p < 0.05$ vs Normal (1.5 h), #, $p < 0.05$ vs Normal (6 h). Two-tailed Student's t test. **b** Rat primary cortical neurons were subjected to OGD for 1.5 h followed by reoxygenation for 0 or 6 h or cultured in normal condition (Normal). MiR-210 level was measured by RT-PCR. Data are expressed as mean ± SEM. $n \geq 3$ independent experiments. *, $p < 0.05$, ***, $p < 0.001$ vs Normal. **, $p < 0.005$ vs 0 h of reoxygenation. ANOVA following by Newman-Keuls post hoc test

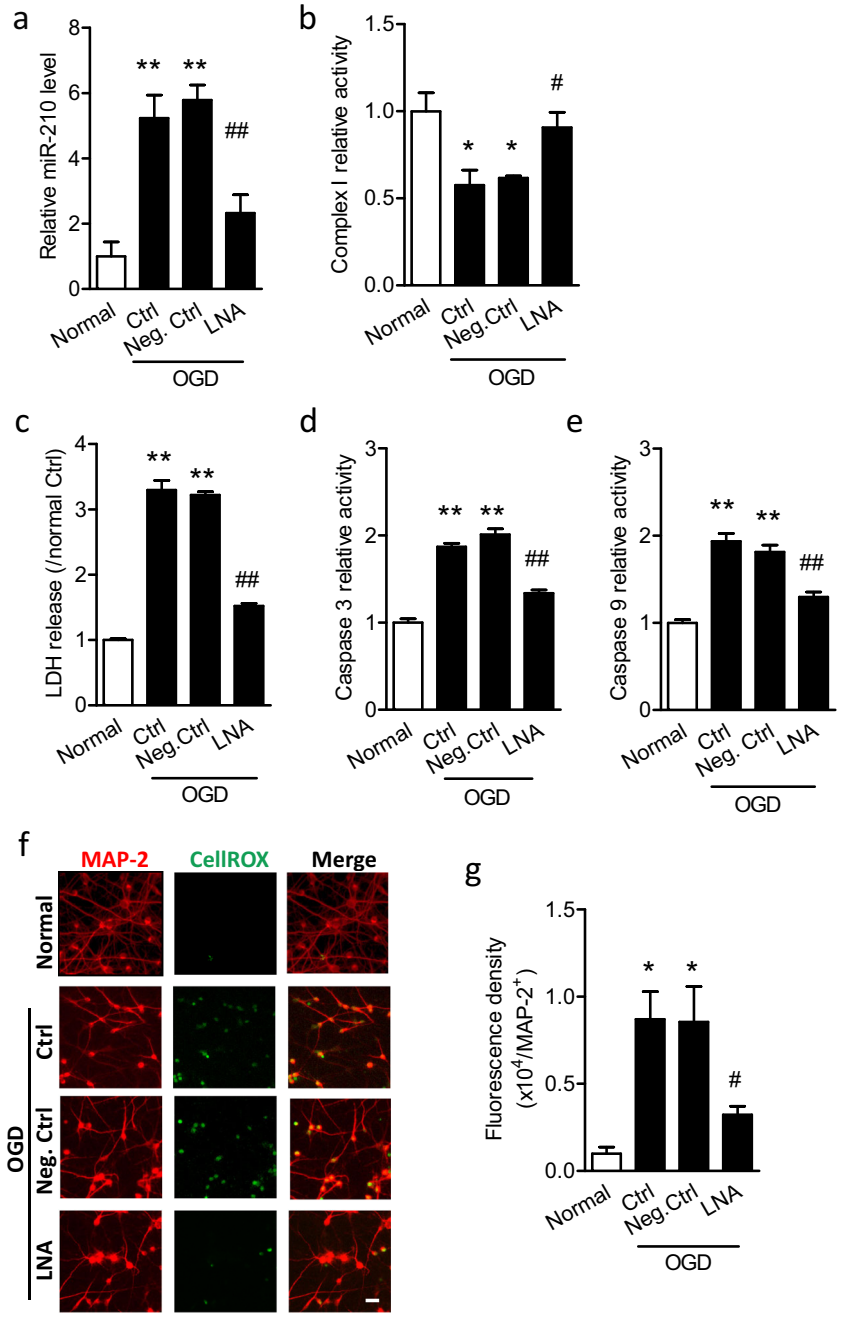

Fig. 3 Inhibition of miR-210-LNA reduces neuronal cell viability and intracellular ROS in primary cortical neurons by downregulation of miR-210 level after OGD/reoxygenation. Rat primary cortical neurons at DIV5–7 were treated with 50 μM miR-210-LNA or scramble LNA (Neg. Ctrl) 24 h, and then were subjected to OGD for 1.5 h followed by reoxygenation. Control cells (normal) were cultured in normal condition for the same durations. **a** RT-PCR for the level of miR-210 6 h after reoxygenation. Data are expressed as mean ± SEM. $n \geq 3$ independent experiments. **, $p < 0.005$, vs Normal; ##, $p < 0.005$ vs LNA. ANOVA following by Newman-Keuls post hoc test. Complex I activity (**b**), LDH release (**c**), caspase 3 activity (**d**), and caspase 9 activity (**e**) were detected at the end of 24 h of reoxygenation. Data are expressed as mean ± SEM. In **b**, $n = 3$ independent experiments. In **c**–**e**, $n = 4$ independent experiments. *, $p < 0.05$, **, $p < 0.005$ vs Normal. #, $p < 0.05$, ##, $p < 0.005$ vs Neg. Ctrl. ANOVA following by Newman-Keuls post hoc test. **f** Representative images of the colocalization of intracellular ROS (CellROX, green) and cortical neurons (MAP 2, red). Scale bar, 20 μm. Rat primary cortical neurons were seeded on PDL-coated 12-mm glass coverslips in 24-well plates. **g** Quantitation of the density of intracellular ROS fluorescence in MAP 2-positive neurons. Data are expressed as mean ± SEM. $n = 4$ independent experiments. *, $p < 0.05$ vs Normal. #, $p < 0.05$ vs Neg. Ctrl. ANOVA following by Newman-Keuls post hoc test

reoxygenation (Fig. 3g). No statistical difference was obtained between OGD alone (Ctrl) and with Neg. Ctrl. Together, these data indicate that miR-210 is stimulated in primary cortical neurons in response to OGD/reoxygenation, and inhibition

of miR-210 blocks mitochondrial dysfunction and intracellular ROS production, resulting in neuroprotection.

MiR-210 Downregulated Mitochondrial ISCU Protein Abundance In Vivo and In Vitro

We further explored whether miR-210 modulated mitochondrial function by downregulating ISCU, which is an established target of miR-210 [20]. Evidence showed that perturbation of the miR-210/ISCU axis resulted in mitochondrial dysfunction and ROS overgeneration in endothelial cells or transformed cells [20, 39]. Yet, its effect in the brain and neurons remains undetermined. We first determined the effect of miR-210 on ISCU protein abundance in the neonatal brain by delivery of either miR-210 mimic or scramble Neg. Ctrl into the right hemisphere in P5 rat pups. Western blot result showed that miR-210 mimic significantly downregulated ISCU protein expression 48 h after injection compared with Neg. Ctrl (Fig. 4a). Furthermore, the HI treatment significantly decreased ISCU protein in mitochondria isolated from the neonatal brain. Of importance, inhibition of brain endogenous miR-210 via *i.c.v.* injection of miR-210-LNA into the ipsilateral hemisphere 4 h after HI significantly blocked the effect of HI and rescued ISCU levels in the mitochondria (Fig. 4b). These in vivo data revealed a causative effect of miR-210 in the HI-induced downregulation of mitochondrial ISCU protein abundance in neonatal brain. Lastly, we determined the direct effect of miR-210 on ISCU abundance in primary cortical neurons. In line with the in vivo results, ISCU protein abundance was significantly decreased in primary cortical neurons after the OGD/reoxygenation treatment, which was rescued in the presence of miR-210-LNA (Fig. 4c).

It has been reported that miR-210 has conserved binding site on the 3′UTR of the ISCU transcript [20]. To determine the causative effect of miR-210 binding to the 3′UTR in downregulation of ISCU, ISCU gene with intact 3′UTR (ISCU-FL) or deletion of 3′UTR (ISCU-3′UTR(−)) was cloned using specific primers and inserted into p3XFLAG-CMV™-7.1 expression vector. To test the expression of Flag-tagged ISCU (Flag-ISCU), plasmids bearing ISCU-FL or ISCU-3′UTR(−) were transfected into PC12 cells. Cells transfected with empty expression vector were used as the control (Ctrl). At 48 h after transfection, strong Flag-ISCU and total ISCU bands were observed in ISCU-FL or ISCU-3′UTR(−) cells using primary antibodies against Flag or ISCU protein, respectively. Accordingly, no Flag-ISCU band and a weak total ISCU band were observed in Ctrl cells (Fig. 5a, left panel). Interestingly, ISCU-3′UTR(−) cells exhibited stronger Flag-ISCU and total ISCU signals than ISCU-FL cells, suggesting the existence of an endogenous negative regulation mechanism of ISCU expression by targeting the 3′UTR. The subsequent immunostaining visualized the expression of Flag-ISCU (green) stained with Flag primary antibody in PC12 cells (DAPI, blue) (Fig. 5a, right panel). Next, to

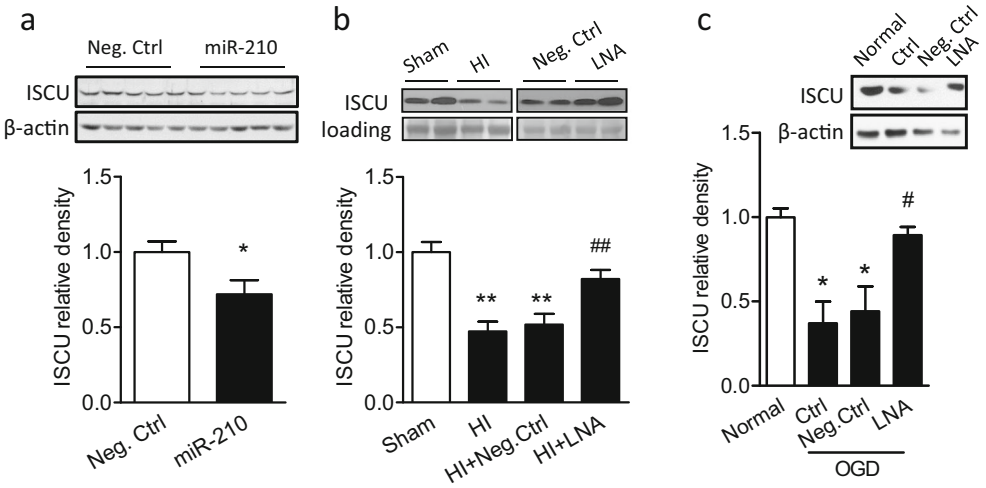

Fig. 4 MiR-210 negatively regulates ISCU expression in vivo and in vitro. **a** miR-210 mimic (100 pmol) or scramble (Neg. Ctrl) was administered into the right hemisphere of P5 rat brain intracerebroventricularly. ISCU protein level was detected by western blots in the ipsilateral cerebral hemisphere of the brain 48 h after injection. Data are expressed as mean ± SEM. $n = 5$ pups/group. *, $p < 0.05$ vs Neg.Ctrl. Two-tailed Student's t test. **b** Neonatal HI brain injury was induced in rat pups, and 100 pmol miR-210-LNA or scramble LNA (Neg. Ctrl) was administered into the ipsilateral hemisphere via *i.c.v.* injection 4 h after HI. ISCU protein level was detected in isolated mitochondria of the ipsilateral cerebral hemisphere of the brain 12 h after HI. Data are expressed as mean ± SEM. $n = 4$ pups/group in Sham and HI; $n = 6$ pups/group in HI + Neg.Ctrl and HI + LNA. **, $p < 0.005$ vs Sham. ##, $p < 0.005$ vs HI + Neg. Ctrl. ANOVA following by Newman-Keuls post hoc test. **c** Rat primary cortical neurons at DIV5–7 were incubated with 50 μM miR-210-LNA or scramble LNA (Neg. Ctrl) 24 h, and then subjected to OGD for 1.5 h followed by reoxygenation. Control cells (Normal) were cultured in normal condition for the same durations. ISCU protein level was detected at the end of reoxygenation. Data are expressed as mean ± SEM. $n = 3$ independent experiments. *, $p < 0.05$ vs Normal. #, $p < 0.05$ vs Neg. Ctrl. ANOVA following by Newman-Keuls post hoc test

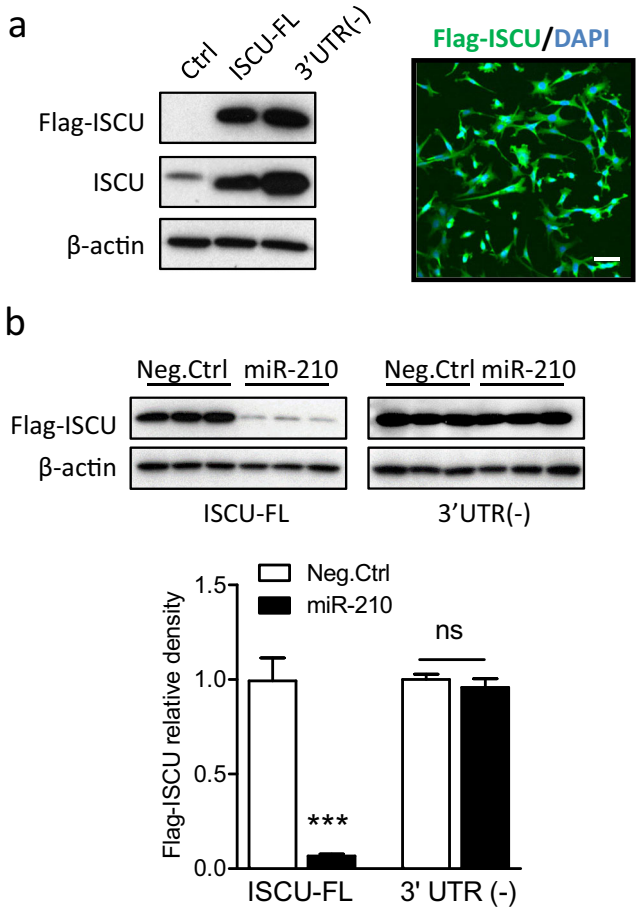

Fig. 5 Deletion of the 3′UTR of the ISCU transcript dampens the regulation of miR-210 on ISCU expression. **a** PC12 cells were transfected with plasmids inserted with ISCU fragments containing intact 3′UTR (ISCU-FL) or deleted 3′UTR (3′UTR(−)), which express Flag-tagged ISCU (Flag-ISCU). Control cells were transfected with empty vectors (Ctrl). **a**, *left panel* Western blots for Flag-ISCU and total ISCU protein levels 48 h after transfection. **a**, *right panel* Representative confocal image of Flag-ISCU expression (green) in PC12 cells (DAPI, blue). Scale bar, 20 μm. **b** Either 100 μM miR-210 mimic or scramble (Neg. Ctrl) was co-transfected with plasmids bearing ISCU-FL or 3′ UTR(−) into PC12 cells. Flag-ISCU and total ISCU protein levels were detected 48 h after transfection. Data are expressed as mean ± SEM. $n = 3$ independent experiments. ***, $p < 0.001$ vs ISCU-FL with Neg.Ctrl. ns, no significant difference. Two-tailed Student's *t* test

validate that miR-210 negatively regulates ISCU by binding to the 3′UTR of the ISCU transcript, either miR-210 mimic or Neg. Ctrl was co-transfected with plasmids of ISCU-FL or ISCU-3′UTR(−) into PC12 cells. In cells transfected with ISCU-FL, the miR-210 mimic treatment resulted in a significant reduction of Flag-ISCU expression, compared with Neg. Ctrl (Fig. 5b, left columns). In contrast, miR-210 mimic had no effect on Flag-ISCU expression in cells transfected with ISCU-3′UTR(−) (Fig. 5b, right columns), demonstrating the requirement of 3′UTR in miR-210-mediated down-regulation of ISCU.

ISCU Knockdown Increased the Vulnerability of the Neonatal Brain to HI and Counteracted the Neuroprotective Effect of miR-210 Inhibition

As the miR-210/ISCU axis was identified both in vivo and in vitro, we then determined the function of ISCU in neonatal HI brain injury. We hypothesized that ISCU knockdown may dampen the neuroprotection of miR-210 inhibition after neonatal HI. To test this hypothesis, first, either ISCU siRNA (si. *Iscu*) or scramble siRNA (si. *Ctrl*) was delivered into the brains of rat pups via *i.c.v.* injection. ISCU mRNA (Fig. 6a) and protein (Fig. 6b) levels were significantly reduced 48 h after the injection of si. *Iscu*, compared with si. *Ctrl*. Interestingly, both miR-210 mimic and ISCU siRNA resulted in a similar degree of ISCU protein loss, that is 38% for miR-210 mimic (Fig. 4a) and 41% to ISCU siRNA (Fig. 6b), suggesting the high selectivity of miR-210-mediated ISCU knockdown. We next determined the effect of ISCU loss on the susceptibility of the neonatal brain to HI. Rat pups were subjected to HI for 1.5 h with prior treatments of either ISCU siRNA or scramble injection, and brain infarct size was detected by TTC staining. Of note, a significant increase of 53% in brain infarct size was observed in si. *Iscu*-treated animals 48 h after HI, compared with si. *Ctrl* (Fig. 6c), revealing a detrimental effect of ISCU downregulation on the neonatal brain. This is in line with the previous observation of miR-210 mimic treatment [16]. Based on this result, we designed a protocol to uncover the role of ISCU in miR-210-LNA mediated neuroprotection. Rat pups were treated with either ISCU siRNA (si. *Iscu*) or scramble (si. *Ctrl*) 48 h prior to the brain HI treatment. Four hours after HI, either miR-210-LNA or scramble LNA (Neg. Ctrl) was delivered into the brain via *i.c.v.* injection, and brain infarction was examined 48 h later by TTC staining. In animals received si. *Ctrl*, miR-210-LNA significantly reduced brain infarct size, compared with Neg. Ctrl (Fig. 6d, left columns). In contrast, in animals pretreated with si. *Iscu*, there was no significant neuroprotective effect of miR-210-LNA in the neonatal HI brain injury (Fig. 6d, right columns). These in vivo results demonstrated the causative effect of ISCU downregulation in miR-210-mediated neonatal brain injury caused by HI treatment.

MiR-210 and ISCU siRNA Mediated Neuronal Mitochondrial Dysfunction, Mitochondrial ROS Overproduction, and Death Signal Activation in Primary Cortical Neurons

We further explored the role of miR-210 and ISCU in regulating mitochondrial functions in primary cortical neurons. Cells at DIV 5 were transfected with 50 μM miR-210 mimic, which significantly reduced ISCU protein abundance (Fig. 7a) and complex I activity (Fig. 7c) 48 h after transfection, compared with Neg. Ctrl. Impairment of complex I activity

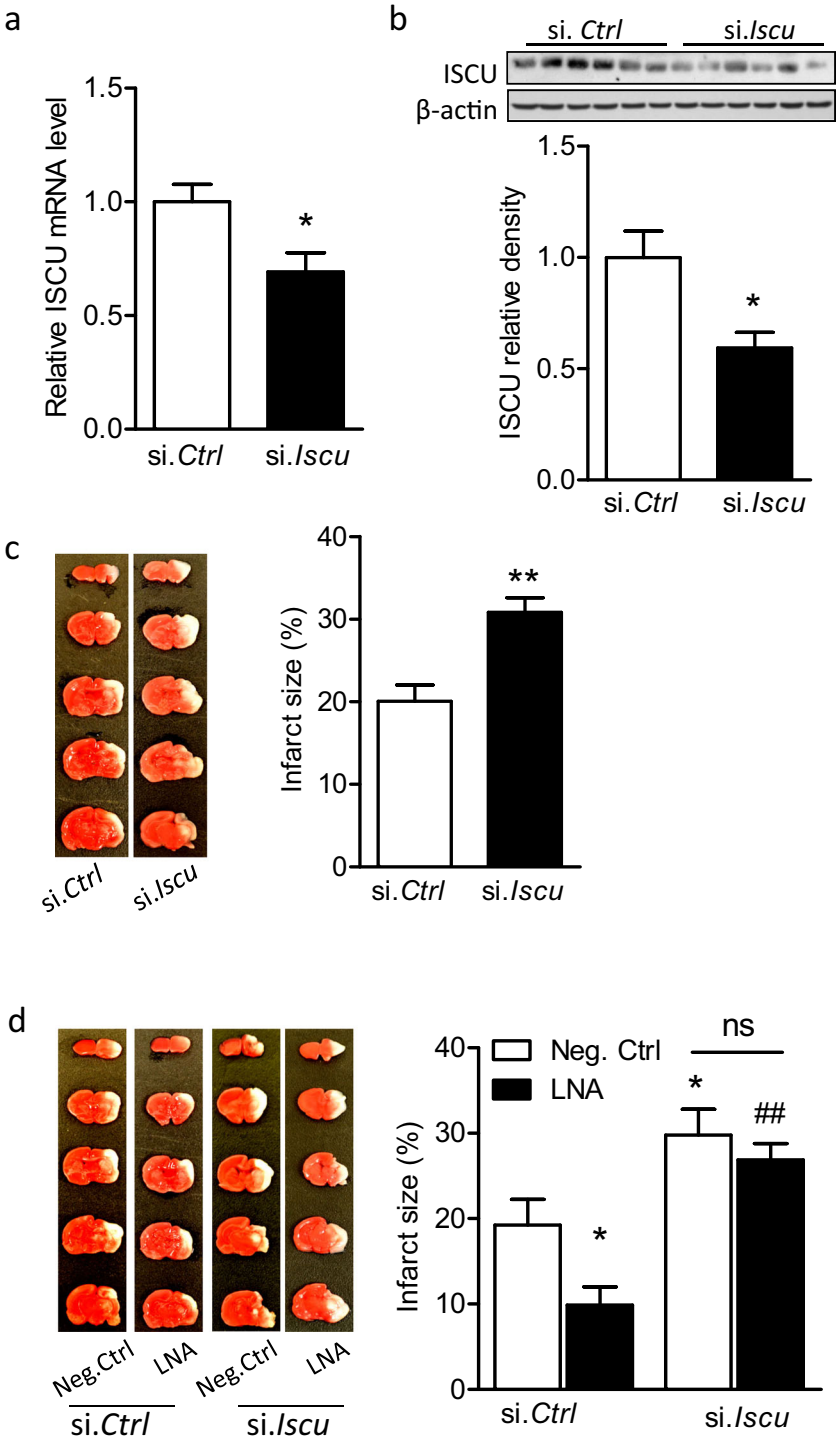

Fig. 6 ISCU knockdown increases the vulnerability of the neonatal brain to HI and counteracts the neuroprotection of miR-210 inhibition. Either ISCU siRNA (100 pmol; si. *Iscu*) or scramble (si. *Ctrl*) was administered into the right hemisphere of rat brain (P5) via *i.c.v.* injection, and 48 h later ISCU mRNA level was detected by RT-PCR (**a**), and protein level was detected by western blot (**b**). Data are expressed as mean ± SEM. $n = 6$ rat pups per group. *, $p < 0.05$ vs si. *Ctrl*. Two-tailed Student's *t* test. **c** Neonatal HI was induced 48 h after ISCU siRNA injection, and brain infarct size was measured by TTC staining 48 h after HI. Data are expressed as mean ± SEM. $n = 10$ pups/group in si. *Ctrl*; $n = 8$ pups/group in si. *Iscu*. **, $p < 0.005$ vs si. *Ctrl*. Two-tailed Student's *t* test. **d** Neonatal HI brain injury was induced 48 h after ISCU siRNA injection, and 4 h later, either 100 pmol miR-210-LNA or scramble LNA (Neg. Ctrl) was administered into the ipsilateral hemisphere of rat brain via *i.c.v.* Brain infarct size was measured by TTC staining 48 h after HI. Data are expressed as mean ± SEM. $n = 6$ pups/group in Neg.Ctrl-treated groups; $n = 8$ pups/group in LNA-treated groups. *, $p < 0.05$ vs Neg.Ctrl-treated si. *Ctrl*. ##, $p < 0.005$ vs miR-210-LNA-treated si. *Ctrl*. ns, no significant difference. ANOVA following by Newman-Keuls post hoc test

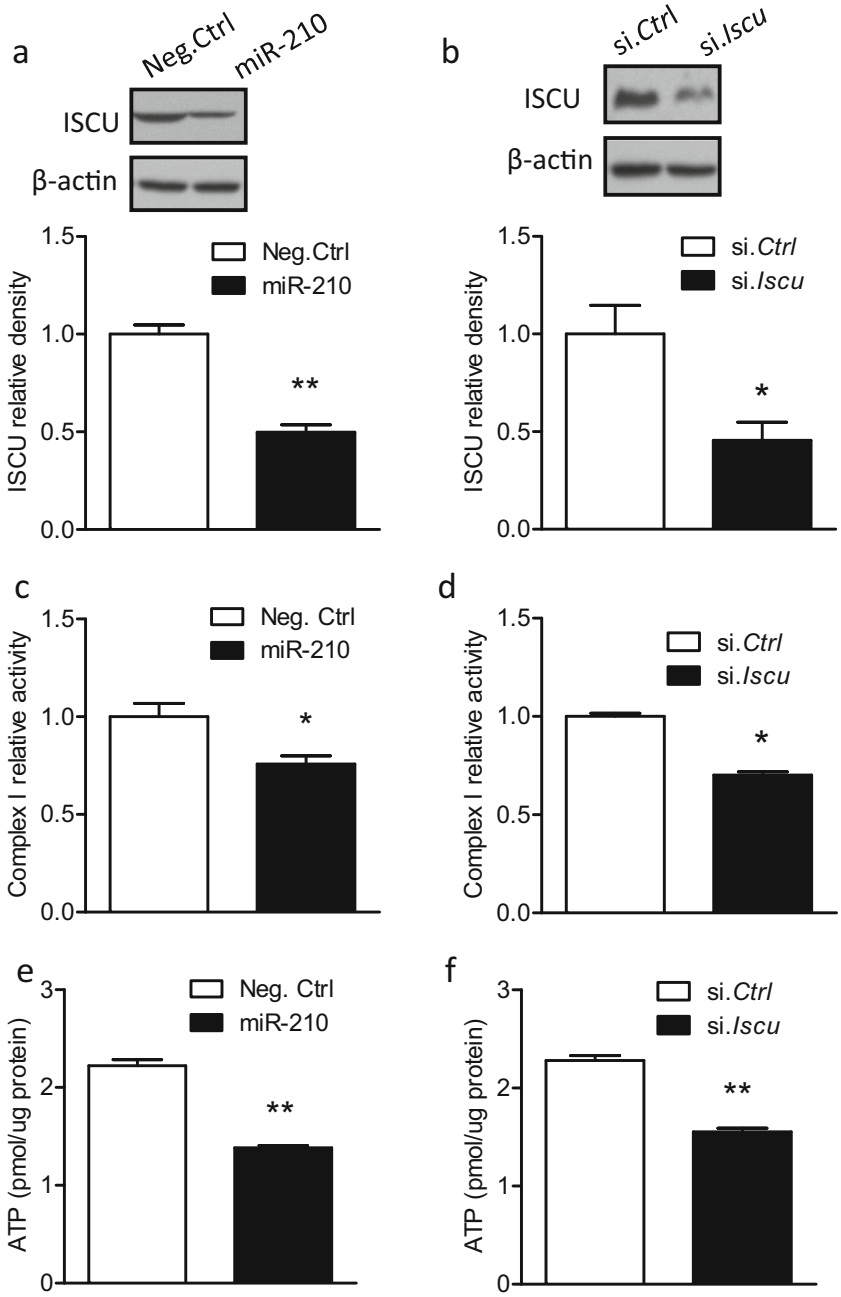

Fig. 7 MiR-210 mimic and ISCU siRNA result in mitochondrial dysfunctions. Rat primary cortical neurons at DIV5 were transfected with 50 μM miR-210 mimic, scramble (Neg. Ctrl), ISCU siRNA (si. *Iscu*), or scramble siRNA (si. *Ctrl*). ISCU protein level (**a**, **b**; western blot), complex I activities (**c**, **d**), and ATP levels (**e**, **f**) were detected after transfection. Data are expressed as mean ± SEM. $n = 3$ independent experiments. *, $p < 0.05$, **, $p < 0.005$ vs Neg. Ctrl or si. *Ctrl*. Two-tailed Student's *t* test

resulted in the disruption of the electron transport and oxidative phosphorylation process, leading to reduction of ATP production [40, 41]. In agreement with these studies, an approximately 38% reduction of ATP levels was observed in cortical neurons with the presence of miR-210 mimic compared with Neg. Ctrl (Fig. 7e). In correlation, cortical neurons transfected with ISCU siRNA also exhibited a reduced ISCU protein expression (Fig. 7b), complex I activity (Fig. 7d) and ATP levels (Fig. 7f). Thus, ISCU siRNA induced the same phenotype in primary cortical neurons as the presence of miR-210 mimic, suggesting that miR-210 and ISCU regulate similar mitochondrial functions.

In regard to the role of miR-210 and ISCU axis in the pathogenesis of neuronal death, we first assessed the mitochondrial ROS using mitochondrial ROS-targeted indicator MitoSOX, which was added into the culture medium at the end of transfection. As expected, increased MitoSOX fluorescence (red) was observed in MAP 2-positive cortical neurons (green) with the presence of miR-210 mimic compared with Neg. Ctrl (Fig. 8a). The overproduction of mitochondrial ROS amplified the intracellular oxidative stress [42–44]. Therefore, the Oxiselect™ in vitro ROS/RNS assay kit was used to measure the levels of intracellular oxidative stress in primary cortical neurons at the end of transfection, which was reflected by

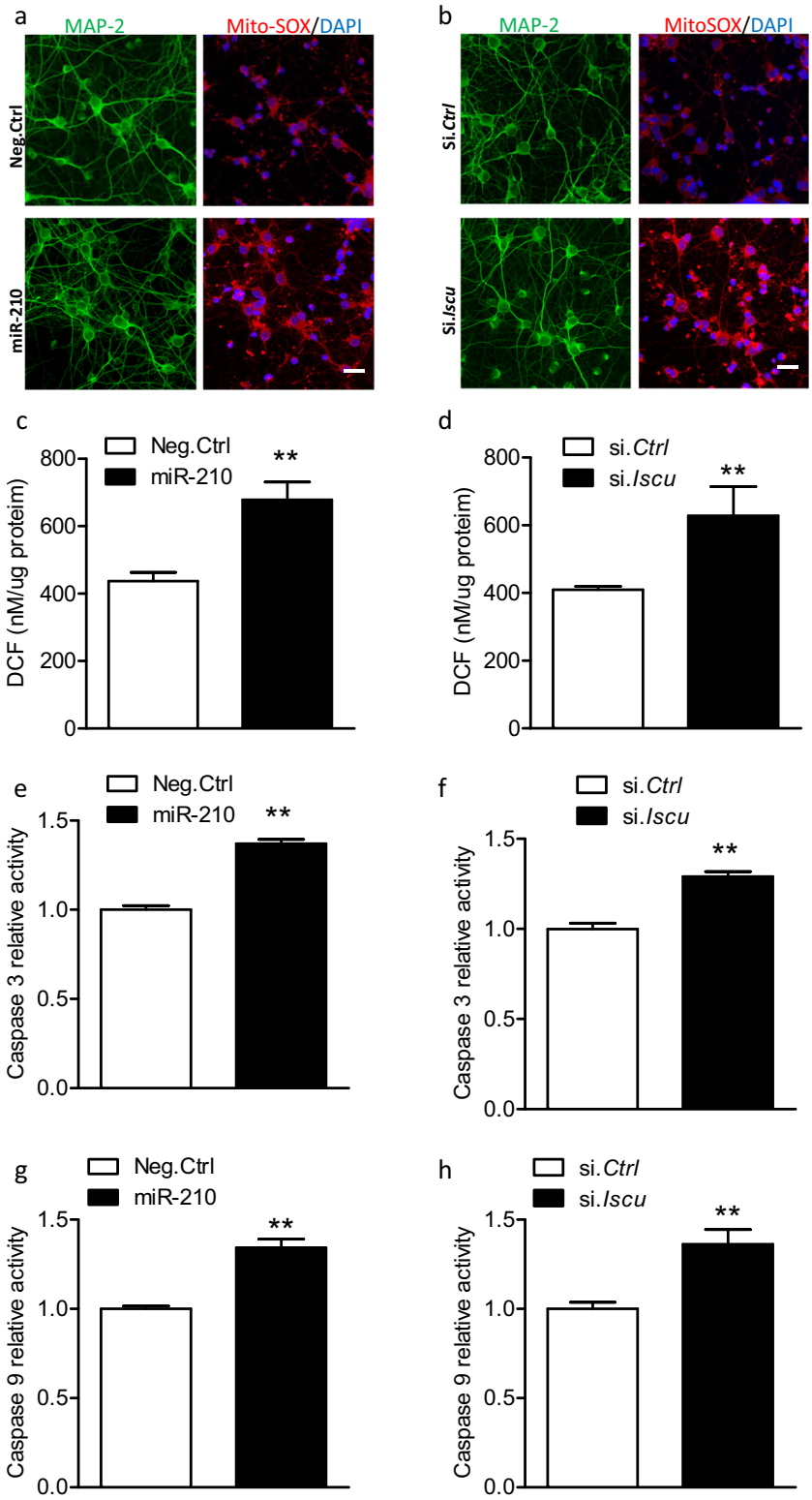

Fig. 8 MiR-210 mimic and ISCU siRNA increase mitochondrial ROS and activated caspase-dependent death pathway. Rat primary cortical neurons at DIV5 were transfected with 50 μM miR-210 mimic, scramble (Neg. Ctrl), ISCU siRNA (si. *Iscu*), or scramble siRNA (si. *Ctrl*). Mitochondrial ROS (**a**, **b**; immunocytochemistry), intracellular ROS (**c**, **d**; DCF), caspase 3 activity (**e**, **f**), and caspase 9 activity (**g**, **h**) were detected 72 h after transfection. In **a**, **b**, representative confocal images of the colocalization of mitochondrial ROS indicator (MitoSOX, red) and cortical neurons (MAP 2; green). Scale bar, 20 μm. Cortical neurons were cultured on PDL-coated 12 mm glass coverslips in 24-well plates. After transfection, cells were washed with pre-warmed growth medium and then incubated with MitoSOX Red at a final concentration of 5 μM for 10 min at 37 °C. Then neurons were briefly washed with PBS followed by immunostaining for neurons (MAP 2) and nuclei (DAPI). In **c**–**h**, data are expressed as mean ± SEM. $n = 3$ independent experiments. **, $p < 0.005$ vs Neg. Ctrl or si. *Ctrl*. Two-tailed Student's *t* test

the levels of highly fluorescent 2′,7′-dichlorofluorescein (DCF), a product oxidized from the oxidant-sensitive fluorophore, 2′,7′-dichlorofluorescin diacetate (DCFDA). The result showed that miR-210 mimic significantly increased DCF fluorescence levels in cortical neurons compared with Neg. Ctrl (Fig. 8c). Furthermore, miR-210 mimic stimulated the caspase-dependent death pathways by showing increased caspase 3 and caspase 9 activities (Fig. 8e, g). Accordingly, similar findings were also observed in the cortical neurons with ISCU knockdown via ISCU siRNA, showing increased

MitoSOX fluorescence (Fig. 8b), intracellular oxidative stress (Fig. 8d), and caspase 3 and caspase 9 activities (Fig. 8f, h). Thus, these data indicate that the miR-210/ISCU axis plays a crucial role in regulating mitochondrial functions, and perturbation of this axis is a major pathogenesis of neuronal death.

Discussion

In term infants, the sensorimotor cortex and the hippocampus are the major regions most vulnerable to HI insults [45, 46]. A series of neurotoxic events, including oxidative stress, inflammatory response, activation of cell death pathways, etc. [47–49], occur within hours and last for days following the onset of HI, ultimately leading to substantial neuronal death and functional deficits [50, 51]. Although multiple pathogenesis have been reported to contribute to HI brain injury, alleviation of neuronal death is still one of the major therapeutic strategies used to treat neonatal HI brain injury [47, 50]. Thus, in the present study, we used a well-established neonatal HI brain injury model in P7 rat pups to investigate the role of miR-210 in brain oxidative injury and neuronal death after neonatal HI. The brain development of P7 rat pup is roughly equivalent to term infants in humans [46, 47]. Therefore, this model can mimic the pathologies, especially neuronal death in infants suffered from HIE. Using this model, we demonstrated that the neuroprotective effect of miR-210 inhibition on neonatal HI brain injury was associated with the preservation of mitochondrial function and the reduction of oxidative stress. Moreover, this neuroprotective effect was further confirmed in primary cortical neurons exposed to OGD/reoxygenation in vitro. We then validated that ISCU was negatively regulated by miR-210 and mediated the effect of miR-210 in the brains of neonates or in primary cortical neurons. Deletion of the 3′ UTR of ISCU transcript blocked the regulation of miR-210 on ISCU expression. Finally, we determined the functions of ISCU in the brain and demonstrated that knockdown of ISCU increased the vulnerability of the neonatal brain to HI and counteracted the neuroprotection of miR-210 inhibition. Specifically, both miR-210 and ISCU modulated multiple functions of mitochondria in primary cortical neurons, and perturbation of the miR-210/ISCU axis resulted in mitochondrial ROS overproduction and activation of caspase-dependent death pathways.

Oxidative stress is one of the major contributors of severe neuronal death and devastating brain damage after neonatal HI brain injury [6, 7]. Generally, oxidative stress is triggered by the disruption of mitochondrial electron transport and oxidative phosphorylation during HI [42–44]. In normal condition, the efficiency of mitochondria relies on the functions of ETC, in which electron transfer from NADH to complex I ensures the ETC activation and the following ATP production. Thus, complex I is one of the major sites of mitochondrial ROS over generation in diverse pathological conditions [52, 53], and therefore regarded as a critical marker indicating mitochondrial dysfunctions. Indeed, mitochondrial complex I activity is reduced after neonatal HI accompanied by an increase in oxidative stress [9]. Given these findings, we detected complex I activity in isolated brain mitochondria in the present study. In agreement with previous studies, HI impaired complex I activity in isolated mitochondria from the neonatal brain, which was rescued by miR-210 inhibition. The same result was obtained in primary cortical neurons with exposure to OGD (Fig. 3b). In addition to ROS production, mitochondrial dysfunction results in generation of reactive nitric species (RNS) that enhance the toxicity of superoxide radicals [54], further disrupt the oxidative metabolism and amplify the excessive generation of mitochondrial free radical species [42]. The accumulation of oxidation products 3-NT and 4-HNE induces neuronal cell death in various CNS disorders related to oxidative stress [34–36]. Therefore, pharmacological antioxidant intervention has been considered as a promising neuroprotection strategy to treat neonatal HI brain injury [6, 7]. To date, some antioxidants, such as allopurinol, melatonin, vitamin E, etc., have been used to provide neuroprotection in term and pre-term HI injury in preclinical studies or clinical trials [7]. In the present study, we found that miR-210 inhibition with miR-210-LNA, which has been demonstrated to be neuroprotection after neonatal HI through either *i.c.v.* or intranasal administration [16], reduced the HI-induced oxidative neuronal injury both in vivo (Fig. 1) and in vitro (Fig. 3). Thus, these results implicate the antioxidant potential of miR-210-LNA in preservation of neuronal mitochondrial function and neuronal survival against HI, and substantiate the mechanism underlying that neuroprotection of miR-210-LNA.

Previously, we demonstrated that miR-210 was time-dependently upregulated in response to HI insults in the neonatal rat brain [16]. In neural stem cell (NSC) cultures, inhibition of miR-210 increased doublecortin (DCX)-positive cell survival under inflammatory conditions associated with improved mitochondrial function [55]. However, the information regarding the expression and function of miR-210 in neural cells, especially neurons, remains limited. In the present study, we found that miR-210 levels were significantly upregulated in primary cortical neurons in response to either short- or long-duration of OGD insult. Moreover, reoxygenation after OGD enhanced the expression of miR-210 (Fig. 3). These results indicate that neuron cells are a major source of miR-210 upregulation in the neonatal brain following HI. MiR-210 is increased by hypoxia in various cell types, including endothelial cells [56], astrocytes [57], and transformed cells [20], etc. Thus, it is

noteworthy that the expression of miR-210 in non-neuronal cells in the brain may also influence neuron viability after neonatal HI in consideration of the complexity of the brain and complicated pathogenesis induced by HI.

We focused on ISCU to reveal the effect of miR-210 in regulating mitochondrial dysfunction in cortical neurons considering the important role of ISCU in mitochondrial energy metabolism, and that ISCU has been demonstrated a target of miR-210 by analysis of luciferase activities with insertion of ISCU 3′UTR fragment into the luciferase reporter constructs [20, 39]. To validate this point, we injected miR-210 mimic into the brains of rat pups and observed a significant reduction of ISCU protein abundance. The same result was obtained in isolated primary cortical neurons with the presence of miR-210 mimic (Fig. 8a) or ISCU silencing siRNA (Fig. 8b). Moreover, the ISCU level was significantly reduced in isolated mitochondria from the neonatal brain in response to HI, as well as in isolated primary cortical neurons in response to OGD, which was reversed by miR-210 inhibition. To reveal the causative effect of miR-210 binding to 3′UTR and ISCU downregulation, we transfected expression plasmids bearing 3′UTR deleted or intact ISCU gene into PC12 cells and found that 3′UTR was required for miR-210-mediated regulation of ISCU expression. These results highlight our findings that the antioxidative effect of miR-210 inhibition is associated with the preservation of complex I activity, for which the function of ISCU is indispensable [21, 58], in both in vivo and in vitro studies.

We then determined the function of miR-210 and ISCU in neonatal HI brain injury. ISCU knockdown increased the vulnerability of the neonatal brain to HI, which was consistent with the previous finding of miR-210 mimic injection [16]. Moreover, ISCU knockdown counteracted the neuroprotective effect of miR-210 inhibition after neonatal HI (Fig. 6d), demonstrating that ISCU is a critical downstream effector in miR-210-mediated neuronal death after HI. ISCU siRNA causes a global knockdown of brain ISCU levels. Therefore, we cannot rule out the indirect effect on neuronal death induced by ISCU knockdown from other cell types after HI brain injury. We further revealed the role of miR-210 and ISCU in the regulation of mitochondrial function in cortical neurons. We observed that complex I activity and ATP levels were significantly reduced, followed by increases in intracellular free species, mitochondrial ROS, and activation of apoptotic cell death signals with either miR-210 treatment or ISCU downregulation by silencing siRNA. These results implicate that miR-210 and ISCU play important roles in maintenance of mitochondrial energy metabolism by regulating multiple functions. In addition to ISCU, we cannot rule out other miR-210 targets such as COX10 (cytochrome c oxidase assembly protein) [39, 55], which may also be involved in the mitochondrial dysfunction, oxidative stress, or cell death after neonatal HI.

Conclusion

In conclusion, the present study demonstrates that inhibition of miR-210 protects against oxidative brain injury with improved mitochondrial function after HI. Using an in vivo neonatal HI model and cultured primary cortical neurons, we uncover the role of miR-210 in regulating mitochondrial function and neuron viability through downregulation of ISCU expression. Of importance, we find that perturbation of miR-210/ISCU axis results in mitochondrial ROS overproduction and activation of death signals in cortical neurons. These findings reveal a causative role of the miR-210/ISCU axis in mitochondria-originated oxidative stress in neurons, and demonstrate the antioxidant potential of miR-210-LNA for the treatment of neuronal death after neonatal HI.

Author Contributions Q.M. and L.Z. contributed to the study design, manuscript preparation, and drafting the manuscript. Q.M., C.D., Y.L., and L.H. contributed to experiment conducting, and data collection and analysis. All authors read and approved the final manuscript.

Funding Information This work was supported by the National Institutes of Health grants HL118861 and NS103017 to L.Z., and American Heart Association Western States Affiliate winter 2015 Beginning Grant-in-Aid 15BGIA25750063 to Q.M.

Compliance with Ethical Standards

Conflict of Interest The authors declare that they have no conflict of interest.

Publisher's Note Springer Nature remains neutral with regard to jurisdictional claims in published maps and institutional affiliations.

References

1. Douglas-Escobar M, Weiss MD (2012) Biomarkers of hypoxic-ischemic encephalopathy in newborns. Front Neurol 3(144). https://doi.org/10.3389/fneur.2012.00144
2. Graham EM, Ruis KA, Hartman AL, Northington FJ, Fox HE (2008) A systematic review of the role of intrapartum hypoxia-ischemia in the causation of neonatal encephalopathy. Am J Obstet Gynecol 199:587–595. https://doi.org/10.1016/j.ajog.2008.06.094
3. Kurinczuk JJ, White-Koning M, Badawi N (2010) Epidemiology of neonatal encephalopathy and hypoxic-ischaemic encephalopathy. Early Hum Dev 86:329–338. https://doi.org/10.1016/j.earlhumdev.2010.05.010
4. Koenigsberger MR (2000) Advances in neonatal neurology: 1950-2000. Rev Neurol 31:202–211
5. Zanelli G, Petrarca M, Cappa P, Castelli E, Berthoz A (2009) Reorientation ability of adults and healthy children submitted to whole body horizontal rotations. Cogn Process 10(Suppl 2): S346–S350. https://doi.org/10.1007/s10339-009-0301-z
6. Johnston MV, Fatemi A, Wilson MA, Northington F (2011) Treatment advances in neonatal neuroprotection and neurointensive care. The Lancet Neurology 10:372–382. https://doi.org/10.1016/S1474-4422(11)70016-3

7. Juul SE, Ferriero DM (2014) Pharmacologic neuroprotective strategies in neonatal brain injury. Clin Perinatol 41:119–131. https://doi.org/10.1016/j.clp.2013.09.004
8. Yin W, Signore AP, Iwai M, Cao G, Gao Y, Chen J (2008) Rapidly increased neuronal mitochondrial biogenesis after hypoxic-ischemic brain injury. Stroke 39:3057–3063. https://doi.org/10.1161/STROKEAHA.108.520114
9. Chavez-Valdez R, Martin LJ, Flock DL, Northington FJ (2012) Necrostatin-1 attenuates mitochondrial dysfunction in neurons and astrocytes following neonatal hypoxia-ischemia. Neuroscience 219:192–203. https://doi.org/10.1016/j.neuroscience.2012.05.002
10. Lu Y, Tucker D, Dong Y, Zhao N, Zhuo X, Zhang Q (2015) Role of mitochondria in neonatal hypoxic-ischemic brain injury. J Neurosci Rehabil 2:1–14
11. Al-Hasan YM, Evans LC, Pinkas GA et al (2013) Chronic hypoxia impairs cytochrome oxidase activity via oxidative stress in selected fetal Guinea pig organs. Reprod Sci 20:299–307. https://doi.org/10.1177/1933719112453509
12. Grivennikova VG, Vinogradov AD (2006) Generation of superoxide by the mitochondrial complex I. Biochim Biophys Acta 1757:553–561. https://doi.org/10.1016/j.bbabio.2006.03.013
13. Kussmaul L, Hirst J (2006) The mechanism of superoxide production by NADH:ubiquinone oxidoreductase (complex I) from bovine heart mitochondria. Proc Natl Acad Sci U S A 103:7607–7612. https://doi.org/10.1073/pnas.0510977103
14. Perier C, Tieu K, Guegan C, Caspersen C, Jackson-Lewis V, Carelli V, Martinuzzi A, Hirano M et al (2005) Complex I deficiency primes Bax-dependent neuronal apoptosis through mitochondrial oxidative damage. Proc Natl Acad Sci U S A 102:19126–19131. https://doi.org/10.1073/pnas.0508215102
15. Lopez-Fabuel I, Le Douce J, Logan A et al (2016) Complex I assembly into supercomplexes determines differential mitochondrial ROS production in neurons and astrocytes. Proc Natl Acad Sci U S A 113:13063–13068. https://doi.org/10.1073/pnas.1613701113
16. Ma Q, Dasgupta C, Li Y, Bajwa NM, Xiong F, Harding B, Hartman R, Zhang L (2016) Inhibition of microRNA-210 provides neuroprotection in hypoxic-ischemic brain injury in neonatal rats. Neurobiol Dis 89:202–212. https://doi.org/10.1016/j.nbd.2016.02.011
17. Esteller M (2011) Non-coding RNAs in human disease. Nat Rev Genet 12:861–874. https://doi.org/10.1038/nrg3074
18. Pasquinelli AE (2012) MicroRNAs and their targets: recognition, regulation and an emerging reciprocal relationship. Nat Rev Genet 13:271–282. https://doi.org/10.1038/nrg3162
19. Nallamshetty S, Chan SY, Loscalzo J (2013) Hypoxia: a master regulator of microRNA biogenesis and activity. Free Radic Biol Med 64:20–30. https://doi.org/10.1016/j.freeradbiomed.2013.05.022
20. Chan SY, Zhang YY, Hemann C, Mahoney CE, Zweier JL, Loscalzo J (2009) MicroRNA-210 controls mitochondrial metabolism during hypoxia by repressing the iron-sulfur cluster assembly proteins ISCU1/2. Cell Metab 10:273–284. https://doi.org/10.1016/j.cmet.2009.08.015
21. Tong WH, Rouault TA (2006) Functions of mitochondrial ISCU and cytosolic ISCU in mammalian iron-sulfur cluster biogenesis and iron homeostasis. Cell Metab 3:199–210. https://doi.org/10.1016/j.cmet.2006.02.003
22. Lee DC, Romero R, Kim JS, Tarca AL, Montenegro D, Pineles BL, Kim E, Lee JH et al (2011) miR-210 targets iron-sulfur cluster scaffold homologue in human trophoblast cell lines: siderosis of interstitial trophoblasts as a novel pathology of preterm preeclampsia and small-for-gestational-age pregnancies. Am J Pathol 179:590–602. https://doi.org/10.1016/j.ajpath.2011.04.035
23. Rice JE, Vannucci RC, Brierley JB (1981) The influence of immaturity on hypoxic-ischemic brain damage in the rat. Ann Neurol 9:131–141. https://doi.org/10.1002/ana.410090206
24. Ma Q, Dasgupta C, Li Y, Huang L, Zhang L (2017) MicroRNA-210 suppresses junction proteins and disrupts blood-brain barrier integrity in neonatal rat hypoxic-ischemic brain injury. Int J Mol Sci 18. https://doi.org/10.3390/ijms18071356
25. Li Y, Xiao D, Dasgupta C, Xiong F, Tong W, Yang S, Zhang L (2012) Perinatal nicotine exposure increases vulnerability of hypoxic-ischemic brain injury in neonatal rats: role of angiotensin II receptors. Stroke 43:2483–2490. https://doi.org/10.1161/STROKEAHA.112.664698
26. Beaudoin GM 3rd, Lee SH, Singh D et al (2012) Culturing pyramidal neurons from the early postnatal mouse hippocampus and cortex. Nat Protoc 7:1741–1754. https://doi.org/10.1038/nprot.2012.099
27. Ma Q, Zhang L (2018) C-type natriuretic peptide functions as an innate neuroprotectant in neonatal hypoxic-ischemic brain injury in mouse via natriuretic peptide receptor 2. Exp Neurol 304:58–66. https://doi.org/10.1016/j.expneurol.2018.02.016
28. Frantseva MV, Carlen PL, El-Beheiry H (1999) A submersion method to induce hypoxic damage in organotypic hippocampal cultures. J Neurosci Methods 89:25–31
29. Newcomb-Fernandez JK, Zhao X, Pike BR, Wang KKW, Kampfl A, Beer R, DeFord SM, Hayes RL (2001) Concurrent assessment of calpain and caspase-3 activation after oxygen-glucose deprivation in primary septo-hippocampal cultures. J Cereb Blood Flow Metab 21:1281–1294. https://doi.org/10.1097/00004647-200111000-00004
30. Yin HZ, Sensi SL, Ogoshi F, Weiss JH (2002) Blockade of Ca2+-permeable AMPA/kainate channels decreases oxygen-glucose deprivation-induced Zn2+ accumulation and neuronal loss in hippocampal pyramidal neurons. J Neurosci 22:1273–1279
31. Zhao X, Strong R, Zhang J, Sun G, Tsien JZ, Cui Z, Grotta JC, Aronowski J (2009) Neuronal PPARgamma deficiency increases susceptibility to brain damage after cerebral ischemia. J Neurosci 29:6186–6195. https://doi.org/10.1523/JNEUROSCI.5857-08.2009
32. Gonzalez-Rodriguez PJ, Xiong F, Li Y, Zhou J, Zhang L (2014) Fetal hypoxia increases vulnerability of hypoxic-ischemic brain injury in neonatal rats: role of glucocorticoid receptors. Neurobiol Dis 65:172–179. https://doi.org/10.1016/j.nbd.2014.01.020
33. Ischiropoulos H (1998) Biological tyrosine nitration: a pathophysiological function of nitric oxide and reactive oxygen species. Arch Biochem Biophys 356:1–11. https://doi.org/10.1006/abbi.1998.0755
34. Dalleau S, Baradat M, Gueraud F, Huc L (2013) Cell death and diseases related to oxidative stress: 4-hydroxynonenal (HNE) in the balance. Cell Death Differ 20:1615–1630. https://doi.org/10.1038/cdd.2013.138
35. Aoyama K, Suh SW, Hamby AM, Liu J, Chan WY, Chen Y, Swanson RA (2006) Neuronal glutathione deficiency and age-dependent neurodegeneration in the EAAC1 deficient mouse. Nat Neurosci 9:119–126. https://doi.org/10.1038/nn1609
36. Blanchard-Fillion B, Prou D, Polydoro M, Spielberg D, Tsika E, Wang Z, Hazen SL, Koval M et al (2006) Metabolism of 3-nitrotyrosine induces apoptotic death in dopaminergic cells. J Neurosci 26:6124–6130. https://doi.org/10.1523/JNEUROSCI.1038-06.2006
37. Zhang W, Liu J, Hu X, Li P, Leak RK, Gao Y, Chen J (2015) N-3 polyunsaturated fatty acids reduce neonatal hypoxic/ischemic brain injury by promoting phosphatidylserine formation and Akt signaling. Stroke 46:2943–2950. https://doi.org/10.1161/STROKEAHA.115.010815
38. Zhao X, Wang H, Sun G, Zhang J, Edwards NJ, Aronowski J (2015) Neuronal interleukin-4 as a modulator of microglial

pathways and ischemic brain damage. J Neurosci 35:11281–11291. https://doi.org/10.1523/JNEUROSCI.1685-15.2015
39. Chen Z, Li Y, Zhang H et al (2010) Hypoxia-regulated microRNA-210 modulates mitochondrial function and decreases ISCU and COX10 expression. Oncogene 29:4362–4368. https://doi.org/10.1038/onc.2010.193
40. Escobar-Khondiker M, Hollerhage M, Muriel MP, Champy P, Bach A, Depienne C, Respondek G, Yamada ES et al (2007) Annonacin, a natural mitochondrial complex I inhibitor, causes tau pathology in cultured neurons. J Neurosci 27:7827–7837. https://doi.org/10.1523/JNEUROSCI.1644-07.2007
41. Imaizumi N, Kwang Lee K, Zhang C, Boelsterli UA (2015) Mechanisms of cell death pathway activation following drug-induced inhibition of mitochondrial complex I. Redox Biol 4:279–288. https://doi.org/10.1016/j.redox.2015.01.005
42. Buonocore G, Groenendaal F (2007) Anti-oxidant strategies. Semin Fetal Neonatal Med 12:287–295. https://doi.org/10.1016/j.siny.2007.01.020
43. Davidson JO, Wassink G, van den Heuij LG, Bennet L, Gunn AJ (2015) Therapeutic hypothermia for neonatal hypoxic-ischemic encephalopathy—where to from here? Front Neurol 6(198). https://doi.org/10.3389/fneur.2015.00198
44. Wu Q, Chen W, Sinha B, Tu Y, Manning S, Thomas N, Zhou S, Jiang H et al (2015) Neuroprotective agents for neonatal hypoxic-ischemic brain injury. Drug Discov Today 20:1372–1381. https://doi.org/10.1016/j.drudis.2015.09.001
45. Folkerth RD (2005) Neuropathologic substrate of cerebral palsy. J Child Neurol 20:940–949
46. Semple BD, Blomgren K, Gimlin K, Ferriero DM, Noble-Haeusslein LJ (2013) Brain development in rodents and humans: identifying benchmarks of maturation and vulnerability to injury across species. Prog Neurobiol 106–107:1–16. https://doi.org/10.1016/j.pneurobio.2013.04.001
47. Han BH, DeMattos RB, Dugan LL et al (2001) Clusterin contributes to caspase-3-independent brain injury following neonatal hypoxia-ischemia. Nat Med 7:338–343. https://doi.org/10.1038/85487
48. Perlman JM (2006) Summary proceedings from the neurology group on hypoxic-ischemic encephalopathy. Pediatrics 117:S28–S33. https://doi.org/10.1542/peds.2005-0620E
49. Northington FJ, Zelaya ME, O'Riordan DP, Blomgren K, Flock DL, Hagberg H, Ferriero DM, Martin LJ (2007) Failure to complete apoptosis following neonatal hypoxia-ischemia manifests as "continuum" phenotype of cell death and occurs with multiple manifestations of mitochondrial dysfunction in rodent forebrain. Neuroscience 149:822–833. https://doi.org/10.1016/j.neuroscience.2007.06.060
50. Hossain MA (2008) Hypoxic-ischemic injury in neonatal brain: involvement of a novel neuronal molecule in neuronal cell death and potential target for neuroprotection. Int J Dev Neurosci 26:93–101. https://doi.org/10.1016/j.ijdevneu.2007.08.013
51. Vasiljevic B, Maglajlic-Djukic S, Gojnic M, Stankovic S, Ignjatovic S, Lutovac D (2011) New insights into the pathogenesis of perinatal hypoxic-ischemic brain injury. Pediatr Int 53:454–462. https://doi.org/10.1111/j.1442-200X.2010.03290.x
52. Turrens JF, Alexandre A, Lehninger AL (1985) Ubisemiquinone is the electron donor for superoxide formation by complex III of heart mitochondria. Arch Biochem Biophys 237:408–414
53. Turrens JF (1997) Superoxide production by the mitochondrial respiratory chain. Biosci Rep 17:3–8
54. Patel RP, McAndrew J, Sellak H, White CR, Jo H, Freeman BA, Darley-Usmar VM (1999) Biological aspects of reactive nitrogen species. Biochim Biophys Acta 1411:385–400
55. Volobouéva LA, Sun X, Xu L, Ouyang YB, Giffard RG (2017) Distinct effects of miR-210 reduction on neurogenesis: increased neuronal survival of inflammation but reduced proliferation associated with mitochondrial enhancement. J Neurosci 37:3072–3084. https://doi.org/10.1523/JNEUROSCI.1777-16.2017
56. Fasanaro P, D'Alessandra Y, Di Stefano V, et al (2008) MicroRNA-210 modulates endothelial cell response to hypoxia and inhibits the receptor tyrosine kinase ligand Ephrin-A3. J Biol Chem 283:15878–15883. https://doi.org/10.1074/jbc.M800731200
57. Ziu M, Fletcher L, Rana S, Jimenez DF, Digicaylioglu M (2011) Temporal differences in microRNA expression patterns in astrocytes and neurons after ischemic injury. PLoS One 6:e14724. https://doi.org/10.1371/journal.pone.0014724
58. Rouault TA, Tong WH (2008) Iron-sulfur cluster biogenesis and human disease. Trends Genet 24:398–407. https://doi.org/10.1016/j.tig.2008.05.008